Available online at www.sciencedirect.com
SCIENCE DIRECT
Journal of Photochemistry and Photobiology A: Chemistry 181 (2006) 394–400
Journal of Photochemistry and Photobiology A:Chemistry
www.elsevier.com/locate/jphotochem

Reordering of polystyrene gel due to multiple swelling in organic vapor Fast transient fluorescence technique study

M. Erdoğan [a], Ö. Pekcan [b,*]

[a] *Department of Physics, University of Balikesir, Balikesir 10100, Turkey*
[b] *Department of Physics, Işık University, Maslak, Istanbul 34389, Turkey*

Received 17 December 2004; received in revised form 19 December 2005; accepted 21 December 2005
Available online 14 March 2006

Abstract

Reordering of disc-shaped polystyrene (PS) gels due to multiple swelling, under organic vapor was studied by using Fast Transient Fluorescence (FTRF) technique. Disc-shaped polystyrene gels were prepared by free radical copolymerization (FRC) of styrene (S) with ethylene glycol dimethacrylate (EGDM) as a crosslinker. Pyrene (P) was introduced as a fluorescence probe during polymerization. Swelling experiments were performed by using P doped PS gels under chloroform vapor. After each swelling step, gels were left to dry in an oven at 30 °C for consecutive reswelling experiments. Decay curves of P were measured and pyrene lifetimes, τ, were determined. It was observed that τ values decreased as swelling recycles were repeated. It was observed that after the fifth swelling step, two different regimes appeared in the swelling processes in PS gels. Swelling time constant, τ_c, and cooperative diffusion coefficients, D_c, were determined by using Li–Tanaka equation for each swelling step in both regimes. It was observed that D_c values decreased up to tenth swelling step and then remained unchanged in both regimes.

Keywords: Reordering; Swelling; Gel; Fast transient fluorescence

1. Introduction

Aging is a quite general phenomenon which occurs in a wide variety of off-equilibrium materials, such as polymer glasses. It could influence the mechanical, rheological and magnetic properties of materials. Solubility and transport of small molecules in polymer glasses are also effected by aging [1]. Therefore, detailed understanding of the aging process is desirable to understand and improve the material quality of polymer glasses.

Several studies related to the aging of polymeric gels have been reported in literature, where corresponding physical quantities are presented. Amylopectin gels, aged for different durations (0–39 days), were used to investigate the effects of aging on diffusion of bovine serum albumin by Fourier Transform Infrared microscopy [2]. It was found that the rate of the diffusion initially decreased rapidly as the aging time is increased. Thereafter, it continued to decrease but more slowly. Polarization-modulated light scattering method was used to study aging process of silica alcogel [3]. The Young's modulus of the gel were monitored over time and it was observed, that the magnitude of the gel modulus increased from the order of 10^3 to 10^6 N/m^2 over several days or weeks. The physical aging of poly(methyl methacrylate) (PMMA) during annealing just below T_g was investigated by using light scattering and oscillating-Differential Scanning Calorimetry techniques. The light scattering intensity was found to decrease monotonously with increasing scattering angle [4]. The angular dependence of the intensity was attributed to the long-range density fluctuation and the time variation of the density fluctuation during the physical aging of PMMA glass. In situ photon transmission technique was performed using UV–vis spectrometer during the multiple swelling of polyacrylamide (PAAm) gel in water [5]. It was observed that the transmitted light intensity decreased continuously as the gel swelled. A sudden increase in the gel relaxation time was observed after the eighth swelling step during multiple swelling of the PAAm gel. Gels prepared from aggregated polystyrene colloids were studied by multispeckle dynamic light scattering technique [6]. These experiments supported full characterization of the evolution of the structure of an aging material, and provided convincing support to the validity and generality of many of the

* Corresponding author. Tel.: +90 216 528 7165; fax: +90 212 285 6386.
E-mail address: pekcan@isikun.edu.tr (Ö. Pekcan).

1010-6030/$ – see front matter © 2005 Elsevier B.V. All rights reserved.
doi:10.1016/j.jphotochem.2005.12.025

universal features. Effect of aging on diffusion and sorption of small molecules in Bisphenol A-polycarbonate polymer glasses was studied by site distribution model [1]. They have shown that a small increase in polymeric free volume due to conditioning resulted in deeper traps for penetrant molecules that gives rise to slowing down of gas diffusion.

Swelling is directly related to the viscoelastic properties of a gel [7]. The gel elasticity and the friction between the network and the solvent play a basic role in the kinetics of gel swelling [8–10]. Since swelling of a gel is a diffusion-limited process, the rate is governed by the diffusion of solvent through a network of polymer and is inversely proportional to the square of the characteristic size of the gel [8,10,11]. The elastic and swelling properties of permanent networks can be understood by considering two opposing effects, the osmotic pressure and the restraining force. Usually the total free energy of a chemically crosslinked network can be seperated into two terms; the bulk and the shear energies. The bulk energy of the system is related to the volume change, which is controlled by diffusion. The shear energy, keeps the gel in shape by minimizing the non-isotropic deformation [12,13]. Li and Tanaka [11] have developed a model where the shear modulus, μ, plays a fundamental role in keeping the gel in shape by coupling of any changes in different directions. This model predicts that the geometry of the gel is an important factor, and swelling is not just a diffusion process.

Several experimental techniques have been employed to study the kinetics of swelling and aging of chemical and physical gels, among which are neutron scattering [14], quasielastic and dynamic light-scattering [6,15], macroscopic experiments [16] and in situ interferometric measurements. For about last two decades, transient fluorescence technique for measuring fluorescence decay has been routinely applied to study many polymeric systems [17,18]. Using this technique, a pyrene derivative was employed as a probe to monitor the polymerization, aging and drying of aluminosilicate gels [19], with peak ratios in emission spectra being monitored during these processes. Steady-state fluorescence measurements on the swelling of gels formed by the free radical copolymerization (FRC) of methyl methacrylate and ethylene glycol dimethacrylate (EGDM) in solution have been reported. A pyrene derivative was used as a fluorescence probe to monitor swelling, desorption and drying in real time during in situ experiments [20,21]. Time-resolved and steady-state fluorescence techniques were employed to study isotactic polystyrene in its gel state [22], where excimer spectra were used to monitor the existence of two different conformations in the gel state of polystyrene. More recently, Fast Transient Fluorescence (FTRF) technique was used for monitoring swelling and drying of PS gels under organic vapor [23].

The focus of present work is to study gel reordering due to multiple swelling at the molecular level by using FTRF technique, where excited P molecules are quenched by the penetrant organic vapor molecules in the range of few angstroms. The penetration of organic vapor molecules into a disc-shaped gels formed by FRC of PS crosslinked with EGDM was studied by using FTRF technique, which measures lifetimes. Fluorescence decay profiles of P were measured when the gel was illuminated directly by the exciting light and they were fitted to the exponential law to obtain lifetimes of P. A Strobe Master System (SMS) (from PTI) was used for lifetime measurements, which are much faster than Phase instruments and a Single Photon Counting (SPC) System. At least hundreds of measurements can be taken. Measuring lifetimes directly provides swelling parameters. It was observed that as a gel swells, lifetimes of P inside the gel decrease, which can be modeled using low quenching Stern–Volmer equation. After the fifth swelling step, two different regimes corresponding to a slow and a fast swelling regime appeared in the swelling of PS gels. The swelling time constant, τ_c, and cooperative diffusion coefficients, D_c, were measured for each swelling step in both regimes using the Li–Tanaka equation. It was observed that D_c values decreased up to tenth swelling step and remained constant after that in both regimes.

2. Kinetics of swelling

Swelling experiments of disc-shaped gels have shown that the relative changes of diameter and thickness are the same, indicating that the gel–swelling processes are not pure diffusional processes. In fact the equality of the relative changes of diameter and thickness comes from the resulting non-zero shear modulus, μ; the change of total shear energy in response to any small change in shape that maintains constant volume element within the gel should be zero. The high friction coefficient, f, between the network and the solvent overdamps the motion of the network, resulting in a diffusion-like relaxation. The equation of the motion of a network element during the swelling can be given by [11]:

$$\frac{\partial \vec{u}}{\partial t} = D_c \vec{\nabla}^2 \vec{u} \tag{1}$$

where $\vec{u}$ is the displacement vector measured from the final equilibrium location after the gel is fully swollen ($u=0$ at $t=\infty$). $D_c = (K+4\mu/3)/f$ is the cooperative diffusion coefficient. Here t denotes the time and K is the bulk modulus. Eq. (1) has been used with some success to study the swelling of gels [8]. However, these studies did not properly treat the shear deformation that occurs within a gel during swelling, and, hence, cannot explain, for example, the isotropic swelling of a cylindrical gel. This shortcoming was due to the shear modulus of the network keeping the system in shape by minimizing the non-isotropic deformation. For a disc-shaped gel, any change in diameter is coupled to a change in thickness. The total energy of a gel can be separated into the bulk energy and the shear energy. The bulk energy is related to the volume change, which is controlled by diffusion. The shear energy, F_{sh}, on the other hand, can be minimized instantly by readjusting the shape of the gel [11].

$$\delta F_{sh} = 0 \tag{2}$$

Each small diffusion process determined by Eq. (1) must be coupled to a small shear process given by Eq. (2), resulting in the following relation for a disc-shaped gel:

$$\frac{u_r(R', t)}{R'} = \frac{u_z(a, t)}{a} \tag{3}$$

where R' is the radius and a is the half thickness of the disc gel at the final equilibrium state of the gel. Eq. (3) indicates that the relative change in shape of the gel is isotropic, i.e. the swelling rates of a disc in the axial (z) and radial (r) directions are the same. Simultaneous solution of Eqs. (1) and (2) provides the following equations for the swelling of a gel disc in axial and radial directions [11].

$$u_z(z,t) = \Delta\frac{z}{a}\sum_n B_n \exp\left(\frac{-t}{\tau_n}\right) \tag{4a}$$

$$u_r(a,t) = \Delta\sum_n B_n \exp\left(\frac{-t}{\tau_n}\right) \tag{4b}$$

where Δ is defined as the total change of the radius of the gel and B_n is the pre-exponential factor, related to the ratio of the shear modulus, μ, to the longitudinal osmotic modulus, $M=(K+4\mu/3)$. Here the axial and the radial displacements are expressed as series of components, each of them decaying exponentially with a time constant, τ_n. The first terms of the expressions are dominant at large t, that is at the last stage of swelling. Eqs. (4a) and (4b) can also be written in terms of vapor mass uptakes W at time t and W_∞ at equilibrium as follows:

$$\frac{W_\infty - W}{W_\infty} = \sum_{n=1}^{\infty} B_n \exp\left(\frac{-t}{\tau_n}\right) \tag{5}$$

called the Li–Tanaka equation. In the limit of large t, or if τ_1 which is the first term in the series called τ_c is much larger than the rest of τ_n, all higher term ($n \geq 2$) in Eq. (5) can be omitted and the swelling kinetics is given by the following relation:

$$\left[1 - \frac{W}{W_\infty}\right] = B_1 \exp\left(\frac{-t_s}{\tau_c}\right) \tag{6}$$

It should be noted from Eq. (5) that $\sum B_n = 1$, therefore B_1 should be less than 1. Hence, once the value of B_1 is obtained, one can determine the value of $R=\mu/M$. Here, we have to note that Eq. (6) can also be obtained by using the theoretical results [11], in the case of $R \to 3/4$ ($\mu/K \to \infty$), time constant $\tau_c \approx (3/4 - R)^{-1}$ goes to infinity and all B_n's go to zero except B_1, which goes to unity. The dependence of B_1 on R for a disc can be found in the literature [11]. τ_c is related to the cooperative diffusion coefficient D_c on the surface of a gel disc by:

$$D_c = \frac{3a^2}{\tau_c \alpha_1^2} \tag{7}$$

where α_1 is a function of R only and is given in the literature [11], and a stands for the half thickness of the gel in the final equilibrium state. Hence, D_c can be calculated.

3. Experiments

EGDM has been commonly used as crosslinker in the synthesis of polymeric networks. The monomer styrene S (Merck) and EGDM (Merck) were freed from the inhibitor by shaking it with a 10% aqueous KOH solution, washing with water, and drying over sodium sulfate. After that the mixture was distilled under reduced pressure over copper chloride. The initiator 2,2′-azobisisobutyrronitrile (AIBN, Merck) was recrystallized twice from methanol.

The samples were deoxygenated by bubbling nitrogen for 10 min, and after that the free radical copolymerization of S with EGDM was performed at $70 \pm 2\,^\circ$C in the presence of 2,2′-azobisisobutyrronitrile (AIBN, 0.26 wt.%) as an initiator. P was added as a fluorescence probe during the gelation process. EGDM and P concentrations were kept as 0.015 vol.% and 4×10^{-4} M, respectively. FRC was monitored by fluorescence intensity, which first increased and then saturated in time during gelation. After the gelations had been completed, the PS gel samples were dried under vacuum for the swelling experiment.

Fluorescence decay experiments were performed with the Photon Technology International (PTI) Strobe Master System. In the strobe or alternatively the pulse sampling technique [24,25] the sample is excited with a pulsed light source. The Photo Multiplier Tube (PMT) is gated or strobed by a voltage pulse that is synchronized with the pulsed light source. The intensity of fluorescence emission is measured in a very narrow time window on each pulse and saved in a computer. The time window is moved after each pulse. The strobe has the effect of turning off the PMT and measuring the emission intensity over a very short time window. When the data has been sampled over the appropriate range of time, a decay curve of fluorescence intensity versus time can be constructed.

In situ swelling experiments were carried out at room temperature in the SMS of PTI, employing a pulsed lamp source (0.5 atm of N_2). Pyrenes were excited at 345 nm and fluorescence decay curves were collected at 395 nm in 2 min durations. The disc-shaped gel sample was placed in a 1 cm × 1 cm quartz cell, where it was attached to one side of a cell by pressing a disc against a thick helical steal wire. The bottom of the quartz cell was filled with chloroform. The vapor–gel system was deoxygenated by bubbling nitrogen for 10 min at room temperature to avoid oxygen quenching processes. After that the cell was sealed against oxygen penetration during swelling experiments, and then was placed in the SMS system where fluorescence decay measurements were performed at 90° angle as shown in Fig. 1. In swelling experiments four identical disc-shaped PS gels were used, which were dried and cut from a cylindrical

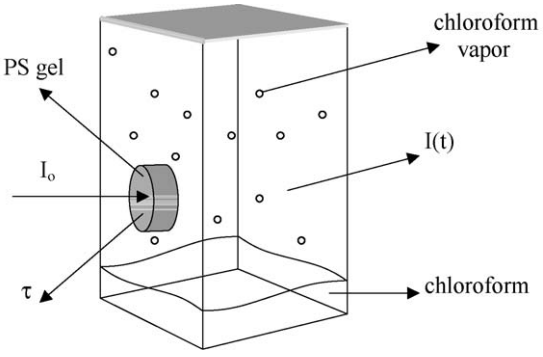

Fig. 1. Fluorescence cell in Strobe Master System. I_0 and $I(t)$ are the excitation and the emission intensities at 345 and 395 nm, respectively. τ is the P lifetime in the gel sample.

Table 1
Swelling parameters of gels

Number of swelling	m_i (g)	m_f (g)	a_i (cm)	a_f (cm)
1	0.076	0.261	0.222	0.260
2	0.090	0.338	0.222	0.270
3	0.093	0.356	0.222	0.275
4	0.087	0.384	0.222	0.275
5	0.092	0.376	0.220	0.270
6	0.089	0.360	0.220	0.270
7	0.097	0.394	0.221	0.286
8	0.099	0.378	0.217	0.278
9	0.089	0.387	0.217	0.280
10	0.086	0.386	0.217	0.278
11	0.088	0.383	0.217	0.285
12	0.087	0.367	0.215	0.275
13	0.088	0.356	0.217	0.285
14	0.086	0.374	0.217	0.285
15	0.088	0.374	0.215	0.280
16	0.088	0.384	0.215	0.270
17	0.087	0.382	0.215	0.275
18	0.087	0.356	0.215	0.280
19	0.087	0.350	0.215	0.270
20	0.087	0.358	0.215	0.275
21	0.088	0.371	0.215	0.280
22	0.088	0.379	0.215	0.275
23	0.087	0.385	0.215	0.278
24	0.087	0.363	0.215	0.270
25	0.087	0.370	0.215	0.275

m_i, a_i and m_f, a_f represent initial weight and thickness and final weight and thickness of the gels, respectively.

gel of radius 0.66 cm that were obtained from FRC with fixed EGDM content. After each swelling step, gels were left to dry in an oven, in air at 30 °C for 4 days until the next reswelling experiment. The fluorescence decay data were collected over 3 time decades, deconvoluted with a dry gel as a scatterer standard and fitted with linear least squares. The uniqueness of the fit of the data to the model is determined by χ^2 ($\chi^2 \leq 1.10$), the distribution of the weighted residuals and the autocorrelation of the residuals. Macroscopic vapor uptake, and disc thickness measurements were performed using a microbalance and callipers, respectively, and results are listed in Table 1.

4. Results and discussions

A typical decay curve of P and the lamp pulse obtained from SMS are shown in Fig. 2. In order to probe the swelling process during vapor uptake, the fluorescence decay curves were measured and were fitted to the following monoexponential functions:

$$I(t) = A\,\mathrm{e}^{-t/\tau} \tag{8}$$

where τ is the pyrene lifetime and A is the corresponding amplitude of the decay curve. In Fig. 3a and b, τ values are plotted versus swelling time, t_s, for the gel sample in its first and tenth swelling steps, respectively. It can be seen that τ values decrease as t_s increases. Here the role of chloroform vapor mass uptake is to add the quasi-continuum of states needed to satisfy energy resonance conditions, i.e. the vapor molecule acts as an energy sink for rapid vibrational relaxation, which occurs after the rate

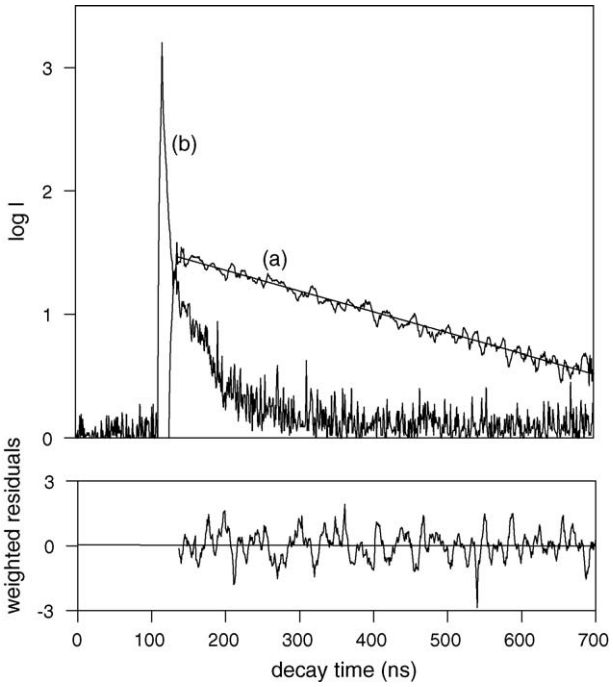

Fig. 2. Fluorescence decay curve (a) of P in PS gel. The light pulse (b) is also shown.

limiting transition from the initial state. Birks et al. studied the influence of solvent viscosity on the fluorescence characteristics of pyrene solutions in various solvents and observed that the rate of monomer internal quenching is affected by solvent quality [26].

Fig. 3a and b exhibit an exponential decrease in τ with increasing swelling time. In order to extract the mass change and the characteristic swelling times, the Stern–Volmer type of quenching mechanism may be proposed for the fluorescence decay of P in the gel sample. According to Stern–Volmer law τ lifetimes can be written as [26]:

$$\tau^{-1} = \tau_0^{-1} + \kappa[W] \tag{9}$$

where τ_0 is the lifetime of P in the dry gel, in which no quenching has taken place, κ the quenching rate constant and $[W]$ is the chloroform vapor concentration in the gel after vapor uptake has started. For low quenching efficiency, ($\tau_0\kappa[W] < 1$), Eq. (9) can be expanded in a series and the following relation is received.

$$\tau \approx \tau_0(1 - \tau_0\kappa[W]) \tag{10}$$

If one integrates Eq. (10) over the differential volume dv of the gel from its initial, a_0, to final thickness, a_f, the following relation is obtained.

$$W = \left(1 - \frac{\tau}{\tau_0}\right)\frac{v}{\kappa\tau_0} \tag{11}$$

Here v is the swollen volume of the gel, which can be measured experimentally for every single swelling step. κ was obtained from separate measurements by using Eq. (11), where the infinity equilibrium value of vapor mass uptake, W_∞, was used. Since τ_0 (≈300 ns) is already known from the dry gel, experimentally measured values of v, W_∞ and τ at equilibrium swelling con-

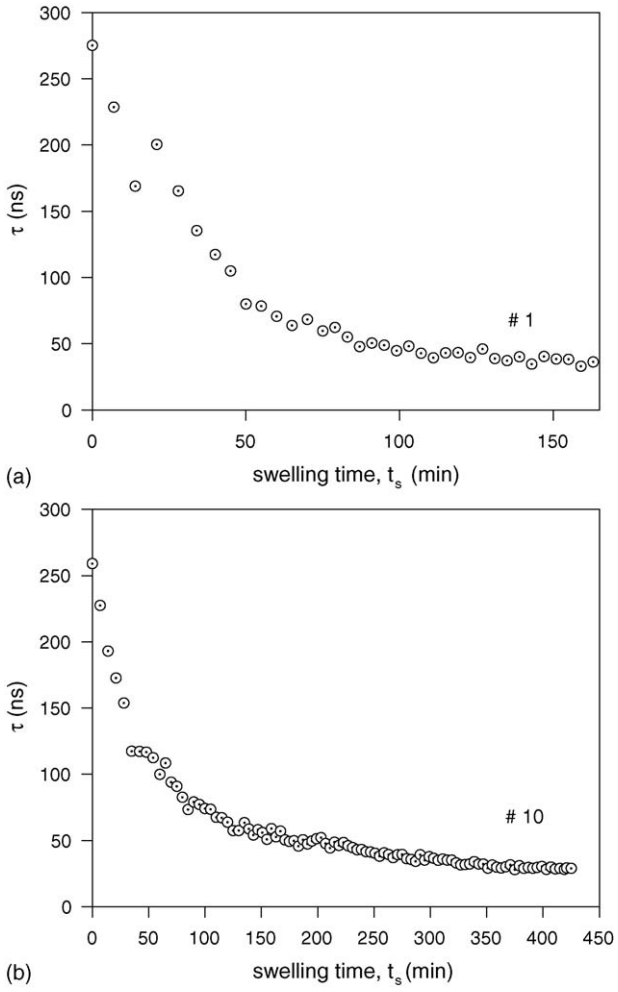

Fig. 3. The plots of the measured τ values vs. swelling time, t_s for the gel sample in first (a) and tenth (b) swelling step.

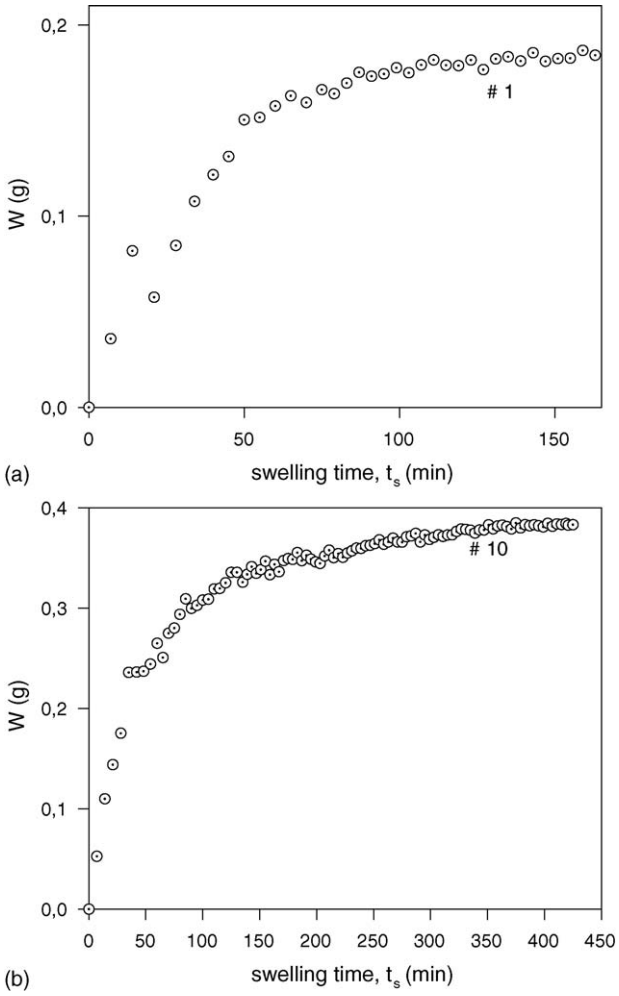

Fig. 4. The plots of the vapor uptake, W vs. swelling time, t_s for the gel sample in first (a) and tenth (b) swelling step.

dition can be used to calculate κ. The value of κ is found to be around 0.9×10^5 cm^3 g^{-1} s^{-1}. Once κ values have been measured, the vapor mass uptakes, W can be calculated from the measured τ values at each swelling step. The plots of the vapor mass uptake, W for the gel sample in its first and tenth swelling steps are presented in Fig. 4a and b, respectively. For the derivation of swelling time constants, we plot the mass uptake of the vapor according to the approximated Li–Tanaka Eq. (6),

$$\ln\left[1 - \frac{W}{W_\infty}\right] = \ln B_1 - \frac{t_s}{\tau_c} \tag{12}$$

versus swelling time, t_s. The results and fits are presented in Fig. 5a and b for the gel sample in its first and tenth swelling steps, respectively. For the first swelling step only one slope is observed, decreasing to the fifth swelling step. For the tenth swelling step, two slopes are found, starting already from the fifth swelling step on. This is consistent with two swelling time constants of about 50 and 100 min, respectively. In other words after the fifth swelling step, PS gel swells in two different regimes, namely fast and slow. The corresponding B_1 and τ_c values were received from linear fits to the different regimes in Fig. 5 as the intercepts and slopes, respectively. The plots of swelling time constants, τ_c and τ_{cs} for long and short time, respectively, swelling regimes versus number of swelling are presented in Fig. 6a. Here full and empty circles represent fast and slow swelling regimes, respectively, which appear after the fifth swelling step. The gray circles at early swelling steps belong to the one-slope regime. There, the penetration of vapor molecules slows down with each consecutive swelling. However, both in the short and long swelling regime, τ_{cs} and τ_c values almost stay constant at all swelling steps. From the calculation of α_1 values with the known B_1 values and from Eq. (7) cooperative diffusion coefficients for both regimes were obtained and are plotted in Fig. 6b versus number of swelling. The behaviour of cooperative diffusion coefficients for both regimes is almost the same. At early swelling steps the D_c values for the non-aged gel decrease. Similarly, the D_{cs} values show a decrease between the fifth and the tenth swelling step. With increasing swelling number, D_c and D_{cs} values above the tenth swelling steps are rather constant.

This behaviour of PS gel may be explained as follows: the increasingly slowing down of swelling at the first fifth swelling steps can be interpreted as a pronounced reordering of the polymer network. After that two independent processes are estab-

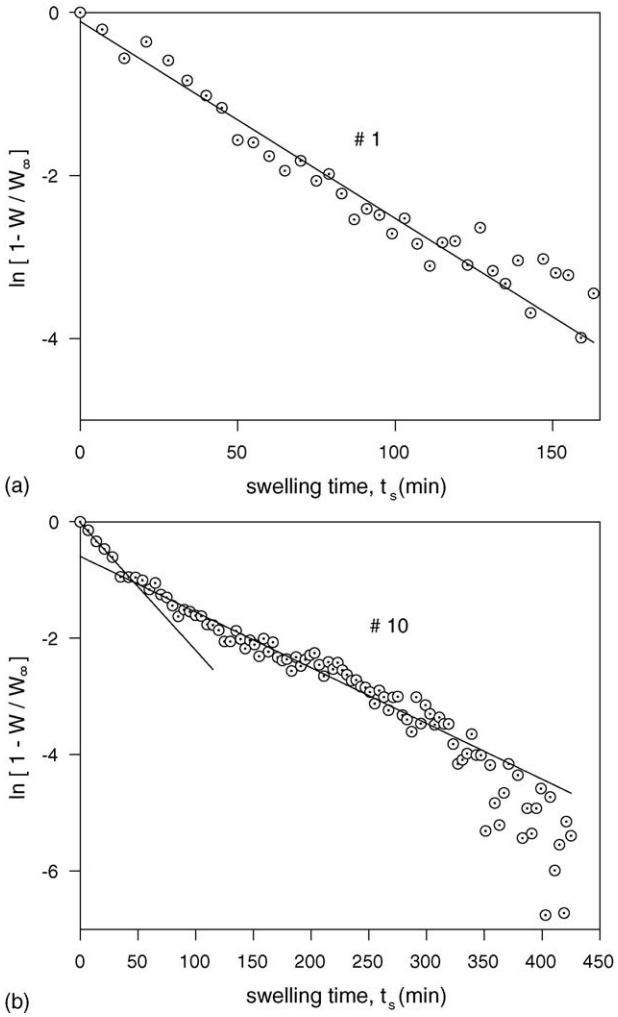

Fig. 5. Fit of the data in Fig. 4 to Eq. (12), where the slope of the straight lines produced τ_c values for the the gel sample in first (a) and tenth (b) swelling step.

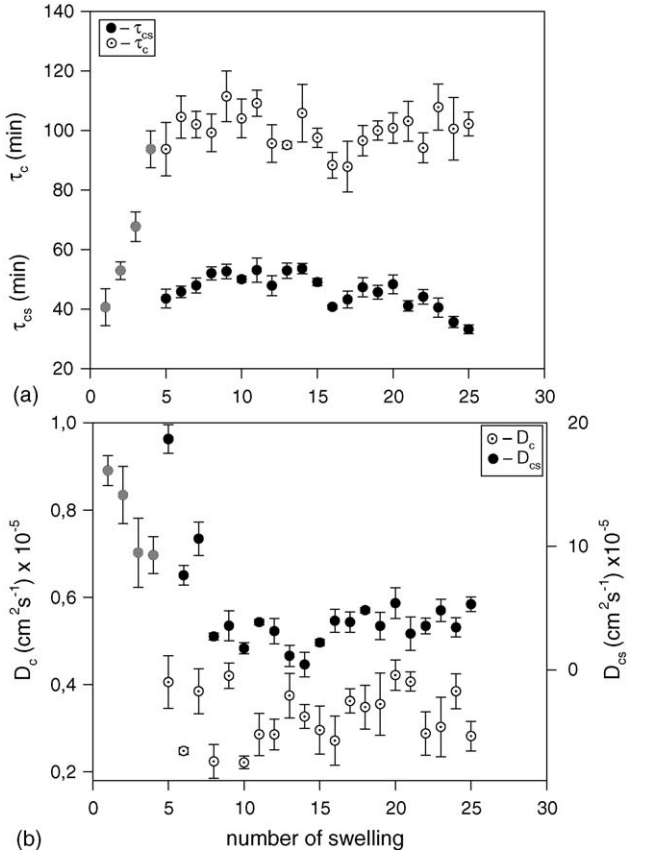

Fig. 6. The plots of: (a) swelling time constants and (b) cooperative diffusion coefficients vs. number of swelling for short and long swelling regimes. τ_{sc} and D_{sc} stand for short and τ_c and D_c stand for long swelling regimes, respectively. The gray circles represent the one-slope regime at early swelling steps.

lished, represented by two well distinguishable swelling time constants and cooperative diffusion coefficients. The slower diffusion process might come from the response of the elastic stresses imposed on the crosslinked gel. The faster diffusion process might be attributed to the swelling of non-crosslinked parts in the gel. Such parts might be entanglements, loops or free volumes. During the first swelling step non-crosslinked parts as entanglements affects the swelling. Consecutive swelling steps, however, reorder the gel, leading to an increasing influence of slow equilibrating elastic forces. These increasingly affect the quenching of pyrene molecules. After reordering is complete, the faster diffusion regime owing to the non-crosslinked parts can be seen again. In other words: the swelling time is more and more affected by the elastic stress without changing the shape of the entangled domains, as long as pronounced reordering occurs. Once, the gel is reordered both diffusion processes are decoupled and can be seen separately.

Several studies related to diffusion of aqueous and non-aqueous agents into polymeric networks have been reported in literature, where corresponding diffusion coefficients are presented. The pulsed field gradient nuclear magnetic resonans (PFG-NMR) technique was used to investigate the size of a polystyrene nanosphere latex, where the observed diffusion coefficients of PS nanosphere was found to be in the order of 10^{-7} cm^2 s^{-1} [27]. NMR relaxation and pulsed-gradient diffusion measurements was used in precipitated silica-filled poly(dimethylsilixane) (PDMS; silicone rubber) after crosslinking and after subsequent devulcanization by intense ultrasound [28]. Diffusion coefficients for this process have been found to be approximately 10^{-7} to 10^{-9} cm^2 s^{-1}. These diffusion coefficients are slightly smaller than the observed values in this work. The difference between literature values and our finding most probably orijinates from the difference between the gel samples which can contain many deffects, i.e. not perfect.

In summary, at the beginning, we are unable to distinguish the existence of two different domains, namely the entangled and the crosslinked parts of the network. Reordering as a result of multiple swelling allowed detecting the two regimes of different swelling time constant, belong to fast and slow. This we interpret as different irreversible and reversible network reordering processes of the gel.

References

[1] P. Pekarski, J. Hampe, I. Böhm, H.G. Brion, R. Kirchheim, Macromolecules 33 (2000) 2192–2199.

[2] L. Sun, A.D. Donald, Int. J. Bio. Macromol. 20 (1997) 205–207.
[3] A.J. Hunt, M.R. Ayers, J. Non-Cryst. Solids 285 (2001) 162–166.
[4] K. Takahara, H. Saito, T. Inoue, Polymer 40 (1999) 3729–3733.
[5] Ö. Pekcan, H. Catalgil-Giz, M. Caliskan, Polymer 39 (1998) 4453–4456.
[6] L. Cipelletti, S. Manley, Phys. Rev. Lett. 84 (2000) 2275–2278.
[7] K. Dusek, Adv. Polym. Sci. 1 (1993) 109.
[8] T. Tanaka, D. Filmore, J. Chem. Phys. 70 (1979) 1214–1218.
[9] A. Peters, S.J. Candau, Macromolecules 19 (1986) 1952–1955.
[10] P. Chiarelli, D. De Rossi, Prog. Colloid Polym. Sci. 78 (1988) 4.
[11] Y. Li, T. Tanaka, J. Chem. Phys. 92 (1990) 1365–1371.
[12] K. Dusek, W. Prins, Adv. Polym. Sci. 6 (1969) 1–102.
[13] S. Candau, J. Bastide, M. Delsanti, Adv. Polym. Sci. 7 (1982) 44.
[14] J. Bastide, R. Duoplessix, C. Picot, S.J. Candau, Macromolecules 17 (1984) 83–93.
[15] A. Peters, S.J. Candau, Macromolecules 21 (1988) 2278–2282.
[16] C. Wu, C.Y. Yang, Macromolecules 27 (1994) 4516.
[17] Ö. Pekcan, M.A. Winnik, L.S. Egan, M.D. Croucher, Macromolecules 16 (1983) 699–702.
[18] Ö. Pekcan, Chem. Phys. Lett. 198 (1992) 20–24.
[19] J.C. Panxviel, B. Dunn, J.J. Zink, J. Phys. Chem. 93 (1989) 2134–2139.
[20] Y. Yilmaz, Ö. Pekcan, Polymer 39 (1998) 5351–5357.
[21] Ö. Pekcan, Y. Yilmaz, in: W. Rettig, B. Strehnnel (Eds.), Applied Fluorescence in Chemistry, Biology and Medicine, Springer-Verlag, Berlin, 1999, p. 331.
[22] B. Wandelt, D.J.S. Birch, R.E. Imhof, A.S. Holmes, R.A. Pethnick, Macromolecules 24 (1991) 5141–5150.
[23] M. Erdogan, Ö. Pekcan, Polymer 45 (2004) 2551–2558.
[24] J.R. Lakowicz, Principles of Fluorescence Spectroscopy, Plenum Press, New York, 1983.
[25] W.R. Ware, D.R. James, A. Siemiarczuk, Rev. Sci. Inst. 63 (1992) 1710–1716.
[26] J.B. Birks, M.D. Lumb, J.H. Mumro, Proc. R. Soc. A 277 (1964) 289–297.
[27] T. Saito, K. Shimada, S. Kinugasa, Langmuir 20 (2004) 4779–4781.
[28] S.E. Shim, I. Isayev, E.V. Meerwall, J. Polym. Sci. Part B: Polym. Phys. 41 (2003) 454–465.